General two-species interacting Lotka-Volterra system: Population dynamics and wave propagation

Haoqi Zhu,[1] Mao-Xiang Wang,[1,*] and Pik-Yin Lai[2,†]

[1]*School of Science, Nanjing University of Science and Technology, Nanjing 210094, China*

[2]*Department of Physics and Center for Complex Systems, National Central University, Chung-Li District, Taoyuan City 320, Taiwan, Republic of China*

(Received 2 February 2018; revised manuscript received 8 May 2018; published 25 May 2018)

The population dynamics of two interacting species modeled by the Lotka-Volterra (LV) model with general parameters that can promote or suppress the other species is studied. It is found that the properties of the two species' isoclines determine the interaction of species, leading to six regimes in the phase diagram of interspecies interaction; i.e., there are six different interspecific relationships described by the LV model. Four regimes allow for nontrivial species coexistence, among which it is found that three of them are stable, namely, weak competition, mutualism, and predator-prey scenarios can lead to win-win coexistence situations. The Lyapunov function for general nontrivial two-species coexistence is also constructed. Furthermore, in the presence of spatial diffusion of the species, the dynamics can lead to steady wavefront propagation and can alter the population map. Propagating wavefront solutions in one dimension are investigated analytically and by numerical solutions. The steady wavefront speeds are obtained analytically via nonlinear dynamics analysis and verified by numerical solutions. In addition to the inter- and intraspecific interaction parameters, the intrinsic speed parameters of each species play a decisive role in species populations and wave properties. In some regimes, both species can copropagate with the same wave speeds in a finite range of parameters. Our results are further discussed in the light of possible biological relevance and ecological implications.

DOI: 10.1103/PhysRevE.97.052413

I. INTRODUCTION

The population of a species is often affected by other species forming an ecological web in nature. Furthermore, the population dynamics of a certain species is strongly dependent on another species that is directly interacting. Such a two-species interacting system has received extensive interest both in theories and in ecological observations. In particular, the Lotka-Volterra (LV) model [1–3] is believed to be an appropriate model to study such an interacting community [4,5]. In addition to population dynamics, LV models have been employed in different contexts, such as evolutionary game theory [6–8], food webs [9], and replicator equations [10]. While the dynamics and stability of the LV system for the case of well-mixed populations have been rather well investigated in some situations, such as competitive, cooperative, and predator-prey interactions by various groups, there is little or no complete study on the system with different possible interaction parameters under a unified description. In addition, the case in which the species can undergo spatial diffusion are much less studied. Motility or diffusive motion can drastically alter the temporal dynamics and spatial patterns, and in some situations traveling wave or directed motion can propagate [11,12]. The spatiotemporal patterns resulting from the inter- and intrainteraction dynamics of two species (or agents) are also of recent interest in other dynamical systems, such as evolutionary game theory [8], replicator dynamics [13], and in general reaction diffusion systems. For example, spatial diffusion can lead to various spatiotemporal pattern formations [14], spiral waves in complex Ginzburg-Landau equations [15], and cooperation patterns in prisoners' dilemma dynamics [16,17].

It is known that for LV model with diffusion, there exists traveling wave solutions propagating from one stationary point to another [18–25]. At first glance, diffusion is a kind of random motion that should not be associated with directed motion. However, nonlinearity resulted from the interactions between the species can produce propagating waves, which travel much faster than the species' diffusional speeds. Such a propagating wavefront represents a progressive replacement of one equilibrium (ahead of the front) by another (behind the front). Moreover, it has been shown that propagating wavefront can exist for the competitve [24] and mutualistic [25] LV system with diffusion. It would be of interest to find out other possible wave dynamics and their properties for species interactions in addition to the competitive and mutualistic ones.

In this paper, we consider the LV model of two interacting species with spatial diffusion and investigate the population dynamics and steady wavefront propagation. One of the aims is to summarize all the interaction types between two species described by the LV model and obtain the phase diagram to provide deeper insights in the interacting mechanism in a two-species community. Another goal is to figure out the conditions and properties of wave propagation in the presence of species diffusion for general species interactions. In particular, we shall classify different dynamical scenarios under a unified phase diagram and investigate the wavefront profiles and wave speeds. Analytical results for the wavefront and waveback speeds are obtained using nonlinear dynamics techniques and

*wangmx@njust.edu.cn

†pylai@phy.ncu.edu.tw

tested with numerical solutions. Our results indicate that the intrinsic speed parameters of the two species play a dominant role in determining the wave properties and speeds of the species. The paper is organized as follows: Sec. II gives the classification results of the general LV population dynamics model in terms of the nullclines and presents the phase diagram classifying six dynamical regimes. The presence of species diffusion is considered in Sec. III, in which some analytical results are presented for the wave speeds using nonlinear dynamical analysis. Section IV presents the steady-state wave profiles and wave speeds in various regimes obtained from numerical solution of the partial differential equations and compared with the analytical results. Section V summarizes our result with possible outlooks and further discusses our findings in terms of the biological relevance and implications on ecology or population strategies.

II. TWO-SPECIES INTERACTING LOTKA-VOLTERRA MODEL

We consider the two-species LV model whose populations are denoted by n_1 and n_2. The population dynamics is described by

$$\begin{aligned} \dot{n}_1 &= r_1 n_1(1 - a_{11}n_1 - a_{12}n_2), \\ \dot{n}_2 &= r_2 n_2(1 - a_{22}n_2 - a_{21}n_1), \end{aligned} \tag{1}$$

where $r_\alpha > 0$ ($\alpha = 1,2$) are the growth rates and species interactions are described by the elements in the matrix $\mathbf{a} \equiv \begin{pmatrix} a_{11} & a_{12} \\ a_{21} & a_{22} \end{pmatrix}$. There are two kinds of interactions among the members in the population: intraspecific and interspecific, which are modeled by the parameters $a_{\alpha\alpha}$ and $a_{\alpha\beta}$ ($\alpha \neq \beta$ throughout this paper unless otherwise stated), respectively. The growth is taken to be logistic with $a_{\alpha\alpha} > 0$ representing intraspecific competition. The interspecific interactions are determined by a_{12} and a_{21}, which in general can take positive or negative values. The environmental carrying capacity is taken to be 1. The competition of the β species to suppress the population of the α species is the case with $a_{\alpha\beta} > 0$ ($\alpha \neq \beta$). However, the interspecific cooperation of the β species in promoting the population of the α species can be modeled with $a_{\alpha\beta} < 0$ and n_α can be > 1 due to the assistance from the β species. For the case in which the species can undergo spatial diffusion, the spatial temporal dynamics (in one-dimension) is described by the time-dependent profiles $n_1(x,t)$ and $n_2(x,t)$, which obey the reaction-diffusion equations

$$\begin{aligned} \frac{\partial n_1}{\partial t} &= d_1 \frac{\partial^2 n_1}{\partial x^2} + r_1 n_1(1 - a_{11}n_1 - a_{12}n_2), \\ \frac{\partial n_2}{\partial t} &= d_2 \frac{\partial^2 n_2}{\partial x^2} + r_2 n_2(1 - a_{22}n_2 - a_{21}n_1), \end{aligned} \tag{2}$$

where $d_\alpha > 0$ ($\alpha = 1,2$) are the diffusion coefficients of the corresponding species. In this paper, we will investigate the interplay between population growth, mobilities, and the interactions among the species, and we will classify the population

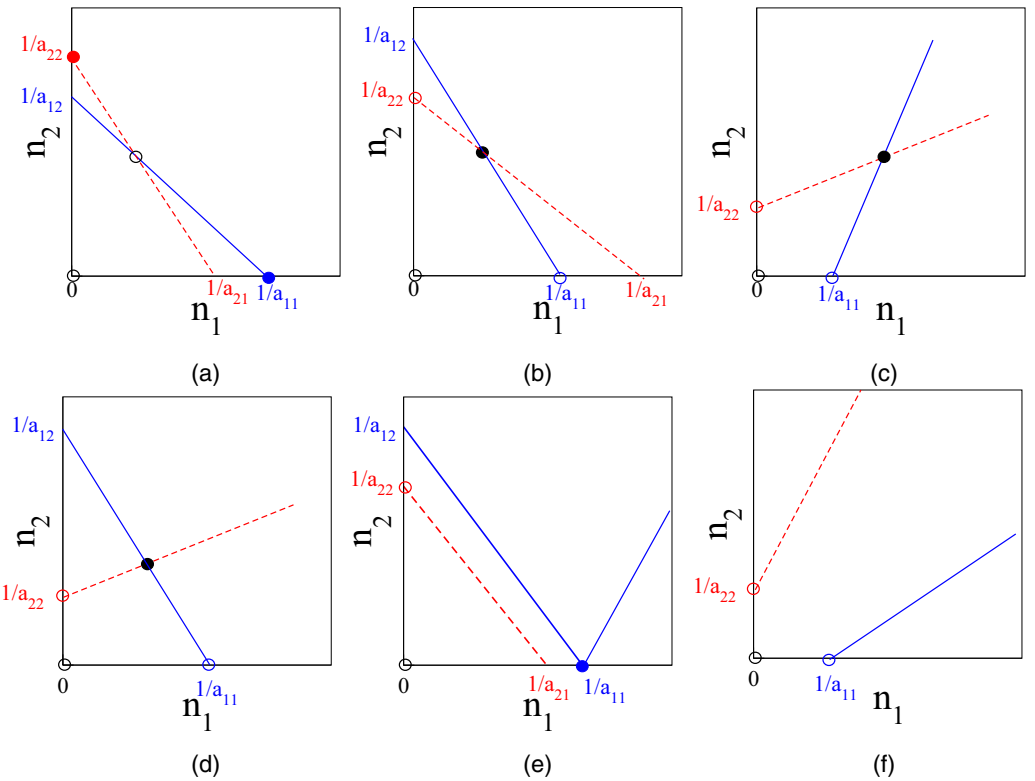

FIG. 1. The nullclines of the kinetic ODE system in Eq. (1) shown in the positive quadrant of the n_1-n_2 phase plane. Solid black and dashed red lines represent the nullclines of species 1 and 2. Stable and unstable fixed points are denoted by • and ○, respectively. (a) Regime I, strong competition; (b) Regime II, weak competition; (c) Regime III, weak mutualism; (d) Regime IV, predator-prey (species 2 is the predator); (e) Regime V, one-species dominating (species 1 is dominating), the slope of the n_1 nullcine (solid line) can be positive or negative as long as the two nullclines do not intersect; (f) Regime VI, strong mutualism.

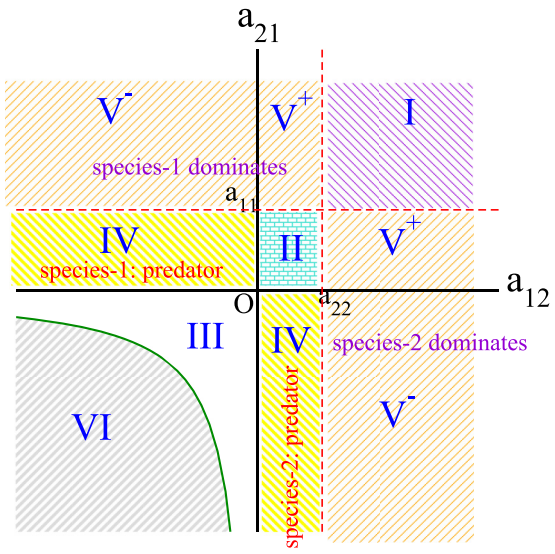

FIG. 2. The phase diagram of two-species interacting Lotka-Volterra model for given intraspecific interactions. The intraspecific interactions are always competitive with both $a_{\alpha\alpha} > 0$. Depending on the properties of the two nullcines, the population dynamics and propagating wave profiles can be classified into six regimes: (I) strong competition regime, (II) weak competition regime, (III) weak mutualism regime, (IV) predator-prey regime, (V) one-species dominating regime, and (VI) strong mutualism regime. In the presence of species diffusion, Regime V can further be subdivided (by the a_{12} or a_{21} axes) into V^+ and V^- regimes. The curve separating Regimes III and VI is given by $a_{12}a_{21} = a_{11}a_{22}$.

dynamics and the associated wave propagations. Some results for the competitive and mutualistic interactions for the special cases of $a_{11} = a_{22} = 1$ have been considered in Refs. [24] and [25], respectively; they are also included here for general values of a_{11} and a_{22} for completeness.

A. Nullclines and homogeneous steady states

Steady states of Eq. (1) occur at the fixed points: (0,0), $(1/a_{11},0)$, $(0,1/a_{22})$, (n_1^*,n_2^*), where $n_1^* \equiv \frac{a_{22}-a_{12}}{\det \mathbf{a}}$ and $n_2^* \equiv \frac{a_{11}-a_{21}}{\det \mathbf{a}}$. Note that the nullcines are two straight lines in the n_1-n_2 phase plane given by

$$a_{12}n_2 = 1 - a_{11}n_1, \tag{3}$$

$$a_{22}n_2 = 1 - a_{21}n_1. \tag{4}$$

The steady state (n_1^*,n_2^*) emerges only when the densities of the populations are nonnegative, i.e., the nullcines have an intersecting point in the first quadrant of the phase plane. Figure 1 shows the possible scenarios in which these two nullcine straight lines within the quadrant of nonnegative densities. As shown in Figs. 1(a)–1(f), these two straight line nullcines can have different slopes that classify the population dynamics and wave properties into six groups, which correspond to six regimes in the phase diagram (see Fig. 2). In the first four cases [Figs. 1(a)–1(d)], the two nullcines intersect inside the positive quadrant giving the nontrivial species coexistence fixed point (n_1^*,n_2^*). Note that Figs. 1(a), 1(b), 1(c), and 1(f) possess $1 \leftrightarrow 2$ exchange symmetry (i.e., topologically invariant under $1 \leftrightarrow 2$). Regimes IV and V include the cases shown in Figs. 1(d) and 1(e), respectively, and their $1 \leftrightarrow 2$ exchange counterparts. The stabilities of the fixed points correspond to the homogeneous steady-state populations can also be obtained easily and are also shown in Fig. 1. Note that the fixed point (0,0) is always unstable. In the strong competition of Regime I, depending on the advantage of its initial population, only one species will survive. Stable coexistence of the two species is possible only in Regimes II, III, and IV, which correspond to the cases of weak competition, weak mutualism, and predator-prey scenarios. In Regime IV, contrary to the conventional predator-prey model [3], in which the predator population can only decay in the absence of the prey, it can be shown that there is no limit cycle oscillation for the populations in this regime of the LV model. For Regime V, the slope of the n_1 nullcine (solid line) can be positive or negative as long as the two nullclines do not intersect. The dominating species will drive the inferior species to extinction. In Regime VI, the two species are too strongly mutually beneficial, which leads to population explosion for both species.

B. The phase diagram

The behavior of various population dynamics and wave profile scenarios can be classified into six regimes as shown in the phase diagram of a_{21} versus a_{12} in Fig. 2. The two species are competitive in the regime when both a_{12} and a_{21} are positive, and they are mutually beneficial if both a_{12} and a_{21} are negative. The population dynamics and propagating wave profiles can be classified into the following six regimes: (I) strong competition, (II) weak competition, (III) weak mutualism (symbiosis), (IV) predator-prey, (V) one-species dominating, and (VI) strong mutualism. Notice that in the presence of species diffusion, Regime V can further be subdivided into two regimes: V^+ (both a_{12} and a_{21} are >0) and V^- (a_{12} and a_{21} are of opposite signs). The curve separating Regimes III and VI is given by $a_{12}a_{21} = a_{11}a_{22}$, with both a_{12} and $a_{21} < 0$. As discussed above, in the absence of diffusion, the ultimate populations are given by the stable fixed point(s) as shown in Fig. 1. Stable two-species coexistence is possible only in Regimes II, III, and IV. However, when the species can migrate and diffuse in space, the intrinsic motilities of the species can alter the fate of the population with the presence of propagating waves. Nevertheless, the system can still be characterized by the same phase diagram in the presence of spatial diffusion, which will be discussed in the following sections.

C. Species coexistence and Lyapunov function

Species coexistence is characterized by the equilibrium populations $n_1^* > 0$ and $n_2^* > 0$, which is present in Regimes I, II, III, and IV. The equilibrium point in Regime I is unstable and stable species coexistence occurs only in Regimes II, III, and IV. The global stability of the coexisting populations in Regimes II, III, and IV (and the unstable coexistence in Regime I) can be described by constructing a single Lyapunov function. As shown in the Appendix, an entropylike Lyapunov

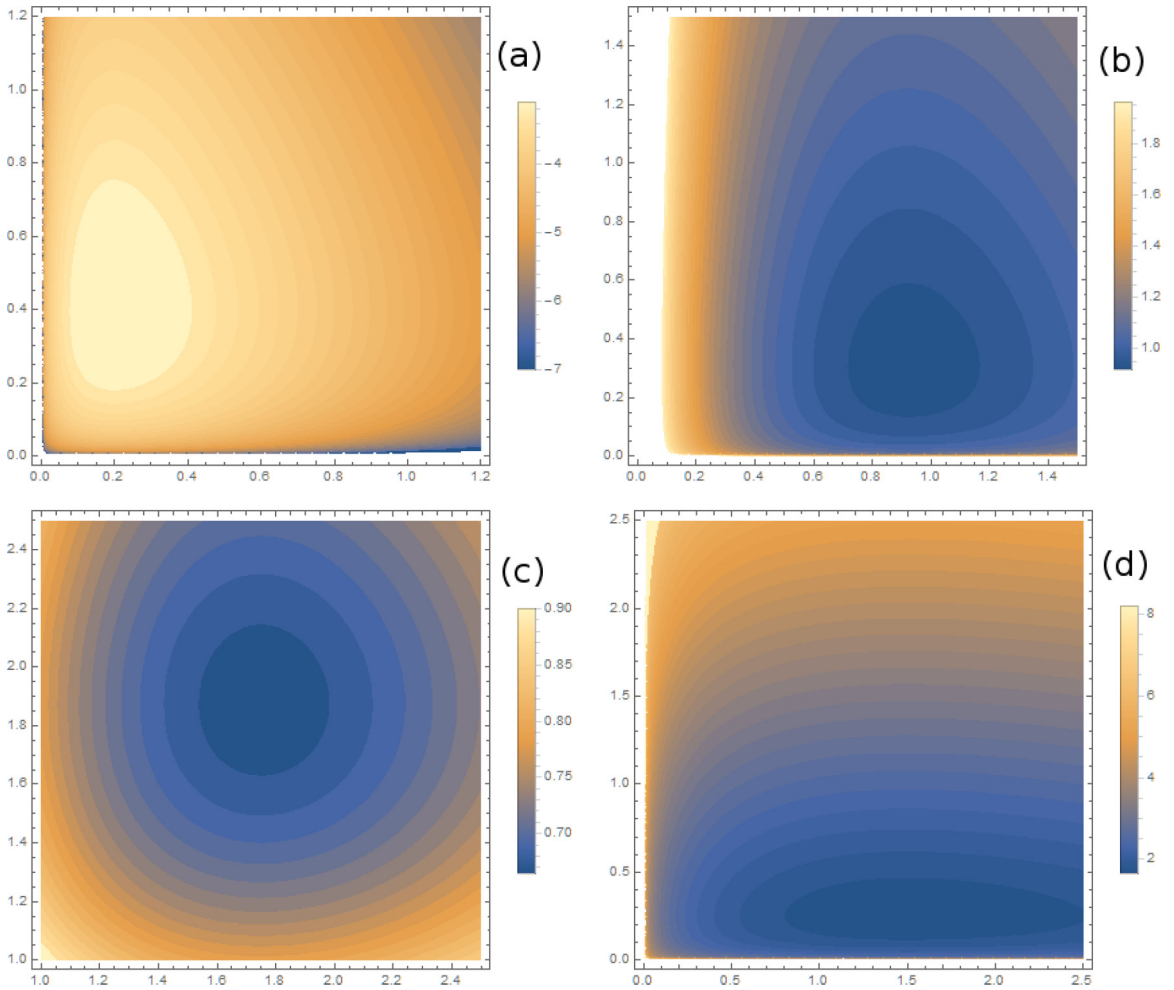

FIG. 3. Lyapunov functions as given by Eq. (5) for species coexistence in various interaction parameter regimes. (a) Regime I for unstable species coexistence due to strong competition; the parameters are the same as in Fig. 5. (b) Regime II for stable species coexistence in the weak competition scenario; the parameters are the same as in Fig. 6. (c) Regime III for stable species coexistence due to weak mutualism; the parameters are the same as in Fig. 7. (d) Regime IV for stable species coexistence in the predator-prey scenario; the parameters are the same as in Fig. 8.

function,

$$V(n_1,n_2) = r_2\mathrm{sgn}(a_{11}-a_{21})|a_{21}|(n_1 - n_1^* \ln n_1) + r_1\mathrm{sgn}(a_{22}-a_{12})|a_{12}|(n_2 - n_2^* \ln n_2), \quad (5)$$

is constructed. In Regimes II, III, and IV, $\dot{V} \leq 0$ everywhere in the n_1-n_2 phase plane with $\dot{V} = 0$ only at (n_1^*,n_2^*), verifying the globally stability of the coexisting populations. Figure 3 shows the Lyapunov functions in these four regimes. V is peak at (n_1^*,n_2^*), indicating its unstable coexistence in Regime I due to strong interspecies competition. The global stability of the species coexistence in Regimes II, III, and IV can be visualized from the minima in V as shown.

III. DIFFUSION OF SPECIES: ANALYTICAL RESULTS FOR WAVE SPEEDS

In this section, the lower bound of wavefront speeds are derived using nonlinear dynamics analysis. Assuming local plane wavefronts with $n_1(x,t) = U_1(x - c_1t)$ and $n_2(x,t) = U_2(x - c_2t)$, then Eqs. (2) are expressed as a four-dimensional first-order ODE system:

$$\begin{aligned} U_1' &= V_1, \\ U_2' &= V_2, \\ d_1V_1' &= -c_1V_1 - r_1U_1(1 - a_{11}U_1 - a_{12}U_2), \\ d_2V_2' &= -c_2V_2 - r_2U_2(1 - a_{22}U_2 - a_{21}U_1). \end{aligned} \quad (6)$$

This four-dimensional ODE system always has three fixed points, $\mathbf{X_0} \equiv (0,0,0,0)$, $\mathbf{X_1} \equiv (1/a_{11},0,0,0)$, $\mathbf{X_2} \equiv (0,1/a_{22},0,0)$, and another fixed point $\mathbf{X_3} \equiv (n_1^*,n_2^*,0,0)$ emerges when both populations are nonnegative. The stability conditions of these fixed points are analyzed by standard nonlinear dynamics techniques, which will give analytical results on the wave speeds.

A. The wavefront speed constraint

In the presence of diffusion, Eqs. (2) resemble the well studied single species Fisher-Kolmogorov-Petrovskii-Piscounov equation [26], which supports propagating wavefront with a constant speed. In this paper, we investigate the stable

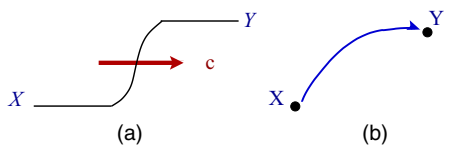

FIG. 4. Schematics illustrating the wavefront propagation for a wavefront obtained by connecting the two homogeneous steady states. (a) Schematic wavefront profile propagating with speed c. (b) Four-dimensional phase space flow from the fixed points **X** to **Y** resulting in a propagating wavefront in (a).

population and the wavefront propagation beyond the simple Fisher's wavefronts for the two species interacting LV model using analytical and numerical means. To begin with, consider a local wavefront that connects two equilibrium states X and Y as shown schematically in Fig. 4(a). For local wavefront solutions propagating in the $+x$ direction, one writes $n_\alpha(x,t) = U_\alpha(x-ct)$, for $\alpha = 1,2$, for some wavefront speed c to be determined. Then the reaction-diffusion-type equations such as Eq. (2) will lead to a system of ODEs with dynamics described by Eq. (6) in a four-dimensional phase space. Two fixed points in the corresponding four-dimensional phase space of the dynamical system are denoted by **X** and **Y**, and a propagating wavefront of speed c is represented by a flow from **X** to **Y** as shown schematically in Fig. 4(b). Suppose the first two components in the phase space vector represent the population profiles, physical requirement requires that these population components to be nonnegative. If the final fixed point **Y** consists of some zero population components, e.g., $\mathbf{Y} = (0,*,*,*)$ or $(*,0,*,*)$, then the flow in phase space when approaching **Y** cannot be an attracting spiral toward **Y**; otherwise, some population components would be negative. The above physical requirement imposes a constraint on the eigenvalue of the Jacobian at **Y** and in turn results in a lower bound on the speed, $c \geqslant c_{\min}$. In many situations (as observed in all the scenarios in this study), the stable wavefront will select to propagate with the minimal speed $c_{\min}$. However, it should be noted that even though a wavefront propagation is possible if there is a flow connecting from **X** to **Y**, the stability of the wavefront is not guaranteed but can be checked by numerical solution of the PDEs.

Furthermore, in all the numerical solution we obtained, for sufficiently sharp initial population profiles, steady wavefront develops and always propagates with its minimal allowed speed. And steady wavefront that propagates with a speed that is not the lower bound value has never been observed. Thus, one can conjecture that all wavefronts will propagate with its minimal constrained limit.

B. Wavefront speeds for the LV model

The eigenvalues of the Jacobian at the fixed point $\mathbf{X_0} \equiv (0,0,0,0)$ obeys $[\lambda(\lambda + \frac{c_1}{d_1}) + \frac{r_1}{d_1}][\lambda(\lambda + \frac{c_2}{d_2}) + \frac{r_2}{d_2}] = 0$, which can be directly computed to give

$$\lambda^{(0)}_{1,\pm} = -\frac{c_1}{2d_1} \pm \sqrt{\left(\frac{c_1}{2d_1}\right)^2 - \frac{r_1}{d_1}},$$
$$\lambda^{(0)}_{2,\pm} = -\frac{c_2}{2d_2} \pm \sqrt{\left(\frac{c_2}{2d_2}\right)^2 - \frac{r_2}{d_2}}, \tag{7}$$

with the corresponding eigenvectors

$$\frac{1}{\sqrt{1+\lambda^{(0)\,2}_{1,\pm}}}\left(1,0,\lambda^{(0)}_{1,\pm},0\right), \qquad \frac{1}{\sqrt{1+\lambda^{(0)\,2}_{2,\pm}}}\left(0,1,0,\lambda^{(0)}_{2,\pm}\right). \tag{8}$$

Contrary to the case of no diffusion in which (0,0) is an unstable fixed point, here all the eigenvalues $\lambda^{(0)}$ have negative real parts and $\mathbf{X_0}$ is stable. Physical requirement demands the fixed point must be a stable node but not a stable spiral; otherwise, regions with negative populations will result. So the wave speeds for wavefront ending with $\mathbf{X_0}$ must exceed the lower bound given by

$$c \geqslant \max[v_1, v_2], \tag{9}$$

where

$$v_\alpha \equiv 2\sqrt{d_\alpha r_\alpha} \qquad \alpha = 1,2 \tag{10}$$

is the intrinsic "speed parameter" of the α species. Notice that the intrinsic wave speed parameter is determined by both the diffusive mobility and the growth rate of the species. It will be shown later that the phase diagrams for the wave profiles and all the wavefront speeds are determined by both the intrinsic speed parameters and the interaction parameters $a_{\alpha\beta}$ of the two species.

For the fixed point $\mathbf{X_1}$, the eigenvalues can be similarly shown to obey $[\lambda(\lambda + \frac{c_1}{d_1}) - \frac{r_1}{d_1}][\lambda(\lambda + \frac{c_2}{d_2}) + \frac{r_2}{d_2}(1 - \frac{a_{21}}{a_{11}})] = 0$, which can be directly computed to give

$$2\lambda^{(1)}_{1,\pm} = -\frac{c_1}{d_1} \pm \sqrt{\left(\frac{c_1}{d_1}\right)^2 + \frac{4r_1}{d_1}}$$
$$2\lambda^{(1)}_{2,\pm} = -\frac{c_2}{d_2} \pm \sqrt{\left(\frac{c_2}{d_2}\right)^2 - \frac{4r_2}{d_2}\left(1 - \frac{a_{21}}{a_{11}}\right)}, \tag{11}$$

with the corresponding eigenvectors

$$\frac{1}{\sqrt{1+\lambda^{(1)\,2}_{1,\pm}}}\left(1,0,\lambda^{(1)}_{1,\pm},0\right), \qquad \frac{1}{\sqrt{1+\lambda^{(1)\,2}_{2,\pm}}}\left(0,1,0,\lambda^{(1)}_{2,\pm}\right). \tag{12}$$

One can see that $\lambda^{(1)}_{1,\pm}$ is always real. For $a_{21} < a_{11}$, there is the possibility of $\mathrm{Im}\{\lambda^{(1)}_{2,\pm}\} \neq 0$ resulting in a spiral. So the physical requirement ensures that $\lambda^{(1)}_{2,\pm}$ must be real leads to

$$c_2 \geqslant \sqrt{(1 - \frac{a_{21}}{a_{11}})}v_2, \qquad \text{for} \quad a_{21} < a_{11}. \tag{13}$$

In this case, the fixed point $\mathbf{X_1}$ is a saddle, which has three stable directions and only one unstable direction. But for $a_{21} > a_{11}$, all eigenvalues are always real with two stable and two unstable eigenvector directions and hence will not set a limit to the wave speed.

Similar analysis applies to $\mathbf{X_2} \equiv (0,1/a_{22},0,0)$ and one can get the eigenvalues and eigenvectors

$$2\lambda^{(2)}_{1,\pm} = -\frac{c_2}{d_2} \pm \sqrt{\left(\frac{c_2}{d_2}\right)^2 + \frac{4r_2}{d_2}},$$
$$2\lambda^{(2)}_{2,\pm} = -\frac{c_1}{d_1} \pm \sqrt{\left(\frac{c_1}{d_1}\right)^2 - \frac{4r_1}{d_1}\left(1 - \frac{a_{12}}{a_{22}}\right)}, \tag{14}$$

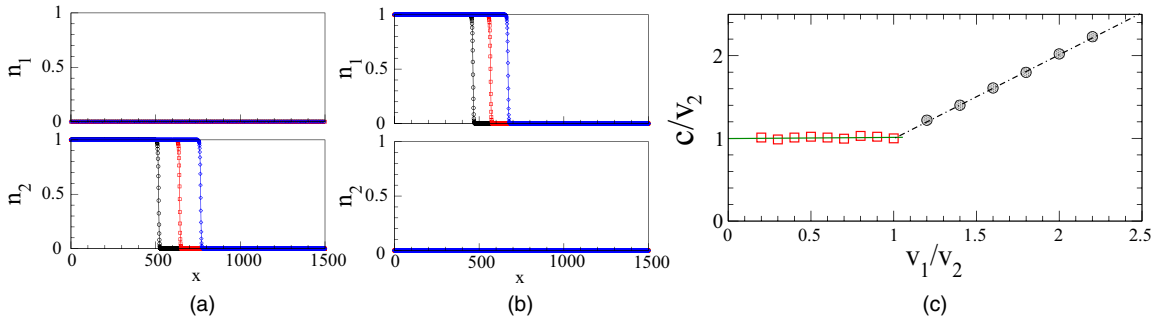

FIG. 5. Steady wavefront profiles in Regime I of the phase diagram Fig. 2 with $a_{12}/a_{22} = 2$ and $a_{21}/a_{11} = 3$, for (a) $v_1/v_2 = 1/2$, (b) $v_1/v_2 = 2$. Three wave profiles each separated by a fixed time difference propagating in the $+x$ direction are shown. (c) Normalized wavefront speeds vs. the speed parameter ratio v_1/v_2. The measured speeds of n_1 and n_2 are denoted by • and □, respectively. Solid and dashed-dotted straight lines are the theoretical minimal speeds given in Eq. (9). Time is in unit of $1/r_1$ and space is in unit of $\sqrt{\frac{d_1}{r_1}}$.

$$\frac{1}{\sqrt{1+\lambda_{1,\pm}^{(2)\,2}}}\left(0,1,0,\lambda_{1,\pm}^{(2)}\right), \qquad \frac{1}{\sqrt{1+\lambda_{2,\pm}^{(2)\,2}}}\left(1,0,\lambda_{2,\pm}^{(2)},0\right). \tag{15}$$

$\mathbf{X_2}$ is also a saddle with three stable directions and one unstable direction for $a_{12} < a_{22}$, and the wave speed constraints of n_1 can be obtained to give

$$c_1 \geqslant \sqrt{\left(1-\frac{a_{12}}{a_{22}}\right)}v_1, \qquad \text{for} \quad a_{12} < a_{22}. \tag{16}$$

And for $a_{12} > a_{22}$, all eigenvalues are real with $\mathbf{X_2}$ having two stable directions and two unstable directions.

As will be illustrated in the next section, the steady wave speeds will always take the minimal values given by the right-hand side of Eqs. (9), (13), and (16). Remarkably, Eqs. (13) and (16) indicate that the wavefront speed of the α species depends not only on the interaction from the other species ($a_{\alpha\beta}$) but also on the intraspecies competition of the other species ($a_{\beta\beta}$). Furthermore, although the wave speed of the α species, c_α, is proportional to its intrinsic speed v_α, it will become vanishingly small as $a_{\alpha\beta} \to a_{\beta\beta}{}^-$. Thus, it would be possible for a species to have a very fast intrinsic speed, but interaction from another species would slow it down indefinitely near the critical value of the interacting parameter, a phenomenon analogous to critical slowing down.

Finally, for the fourth fixed point $\mathbf{X_3}$, the eigenvalues cannot be expressed analytically, but they are given by the solution of the quartic equation

$$\begin{aligned}&\lambda^2\left(\lambda+\frac{c_1}{d_1}\right)\left(\lambda+\frac{c_2}{d_2}\right)+\frac{r_1a_{11}(a_{12}-a_{22})}{d_1\det\mathbf{a}}\lambda\left(\lambda+\frac{c_2}{d_2}\right)\\&+\frac{r_2a_{22}(a_{21}-a_{11})}{d_2\det\mathbf{a}}\lambda(\lambda+\frac{c_1}{d_1})\\&+\frac{r_1r_2(a_{12}-a_{22})(a_{21}-a_{11})}{d_1d_2\det\mathbf{a}}=0,\end{aligned} \tag{17}$$

and the values of the eigenvalues and eigenvectors can be precisely obtained numerically. From the analysis of the eigenvalues, $\mathbf{X_3}$ does not set a limit to the wave speed, but the wave solution connecting these fixed points can become more complicated if $\mathbf{X_3}$ emerges. The steady wavefront profiles are examined in the next section by solving the PDEs in Eq. (2) numerically, with the steady wave speeds also measured.

IV. STEADY WAVE PROFILES AND WAVE SPEEDS IN VARIOUS REGIMES: NUMERICAL RESULTS

According to the phase plane analysis for the nondiffusive LV model, there are six different situations according to the slopes of the nullclines and whether there is an intersection in the positive quadrant. The wavefront profiles are examined by numerically solving the PDEs in Eq. (2) for different regimes in the phase diagram and the steady wave speeds are also measured. Open boundary conditions are used. For convenience, time is in unit of $1/r_1$ and space is in unit of $\sqrt{\frac{d_1}{r_1}}$ in these numerical results. In all cases, the steady propagating wave profiles are determined by the interaction parameters and the intrinsic speed parameters of the two species.

(I) Strong competition, $a_{\alpha\beta} > a_{\beta\beta}$: In this region the competing interaction from the other species is larger than the intraspecific one. Both species are too aggressive and there is only one species that can eventually survive. In the absence of spatial diffusion, the surviving species is determined by its initial population advantage. On the contrary, the situation is quite different in the presence of their diffusive motion. The wave profiles of both species at three different times separated by equal intervals are shown in Figs. 5(a) and 5(b), which correspond to the dynamical situations given by $\mathbf{X_1} \to \mathbf{X_0}$ for $v_1 > v_2$ and $\mathbf{X_2} \to \mathbf{X_0}$ for $v_1 < v_2$, respectively. The deciding factor that determines the ultimate survivors will switch to the intrinsic speed ($v_\alpha \equiv 2\sqrt{d_\alpha r_\alpha}$) of the species in the presence of diffusion. The winner species is the one that possesses a faster v_α. Even if the initial population of the fast species is low, its fast propagating wave speed enables them to escape to regions with no competitors and thus can grow to a dominant population to wipe out the competitors. The wave speeds are also measured from the numerical solutions of Eq. (2) for waves that have attained their steady shapes and are shown in Fig. 5(c) as a function of the ratio of the intrinsic speed parameters, showing that the wave indeed propagates at the minimal speed given by Eq. (9), as claimed in Sec. III.

(II) Weak competition, $0 < a_{\alpha\beta} < a_{\beta\beta}$: In this case, the competing interaction of the other species is weaker than the

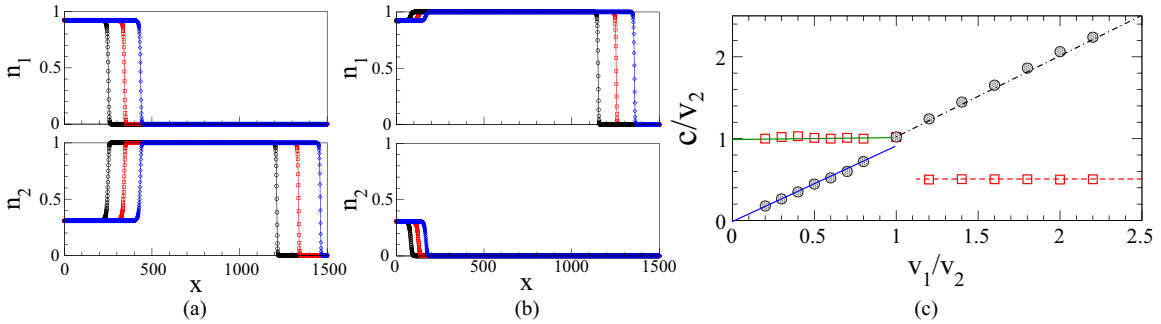

FIG. 6. Steady wavefront profiles in Regime II of the phase diagram Fig. 2 for (a) $v_1/v_2 = 1/2$ and (b) $v_1/v_2 = 2$. (c) Normalized wavefront speeds vs. the speed parameter ratio v_1/v_2. Horizontal solid and dashed-dotted straight lines are the theoretical minimal speeds given in Eq. (9). Solid and horizontal dashed lines are the theoretical minimal speeds given in Eqs. (16) and (13), respectively. $a_{12}/a_{22} = 1/4$, $a_{21}/a_{11} = 3/4$. Symbols and units are the same as in Fig. 5.

intraspecific competition. In the absence of diffusion, both species can coexist persistently, which can be seen from the fact that the intersection of the two nullclines in Fig. 1(b) is a globally stable fixed point [see also Fig. 3(b)]. Such competitive-coexistence scenario persists regardless of the presence of diffusion. In the presence of diffusion, species coexistence remained alongside with the propagation of wavefronts. Figures 6(a) and 6(b) show the wave profiles of the two species at three different times for $v_1 > v_2$ and for $v_1 < v_2$, corresponding, respectively, to the dynamics described by $\mathbf{X_3} \to \mathbf{X_2} \to \mathbf{X_0}$ and $\mathbf{X_3} \to \mathbf{X_1} \to \mathbf{X_0}$. The wavefront ends at the fixed point $\mathbf{X_0}$, which determines the fast propagating speeds similar to the previous case. But now the wavefront profile starts from the new fixed point $\mathbf{X_3}$ instead and passes through the fixed points $\mathbf{X_1}$ or $\mathbf{X_2}$, which in turn sets the wave speed limit of the slower waveback (trailing edge) [given by the lower bounds of Eqs. (13) and (16), respectively]. The wave profiles for the two species are different and determined by their intrinsic speed parameters. The faster species can propagate into regions with no competitors with a wavefront speed given by Eq. (9) and achieving full environmental carrying capacity, but some of its population still lies in regions that coexist with the competitors and hence having a lower (coexisting) population. This is manifested as a waveback for the profile traveling with a speed identical to the wave speed of its competitors.

The steady wavefront propagating speeds for both species are examined as functions of their speed parameter ratio as shown in Fig. 6(c). Similar to the previous case, the nature of the propagating waves show a sharp change as v_1 increases across v_2. The wavefront speeds are also well predicted by minimal speed values from the analytic results in Sec. III. Notice that there is a jump in the wavefront speed of $\delta c_1 = v_1(1 - \sqrt{1 - \frac{a_{12}}{a_{22}}})$ for species 1 and a speed drop of $\delta c_2 = v_2(1 - \sqrt{1 - \frac{a_{21}}{a_{11}}})$ for species 2, as v_1 increases across v_2 [see Fig. 6(c)]. It is worth noting that such a "shift of gears" in the abrupt change of wavefront speeds has also been observed in reaction diffusion cell lineage models involving cell differentiation [27,28].

(III) Weak mutualism, $a_{\alpha\beta} < 0$ and $\det \mathbf{a} > 0$: In this regime, both a_{12} and a_{21} are negative and the strengths of such mutualistic interactions are smaller than the intracompetitions, namely, $a_{12}a_{21} < a_{11}a_{22}$. Commensalism corresponds to the special case of $a_{\alpha\beta} < 0$ and $a_{\beta\alpha} = 0$ in which the β species is beneficial to the α species but is unaffected by the α species. In the absence of diffusion, the species coexistence fixed point [see Figs. 1(c) and 3(c)] is also globally stable. In the presence of such mutual beneficial interactions, the environment capacities of the both species are boosted to high values. However, in the presence of diffusive motion which leads to wave propagation, the faster species may not be able take advantage of the mutualism if it travels too fast into regions with only its own species. Figures 7(a)–7(c) show the wave profiles of the two species at three different times in three speed ratio parameters, corresponding to the regimes of (a) $0 < \frac{v_1}{v_2} \leq \frac{1}{\sqrt{1+\frac{|a_{12}|}{a_{22}}}}$, (b) $\frac{1}{\sqrt{1+\frac{|a_{12}|}{a_{22}}}} < \frac{v_1}{v_2} < \sqrt{1+\frac{|a_{21}|}{a_{11}}}$, and (c) $\sqrt{1+\frac{|a_{21}|}{a_{11}}} \leq \frac{v_1}{v_2}$. In Regimes (a) and (c), the wave profile of the faster species consists of a fast and a slower wavefronts, the slower wavefront has a higher population capacity taking advantage of the mutualistic coexistence of the slower species which travel with the same wavefront speed. Remarkably, there exists a finite regime [Regime (b) above] in which the intrinsic speeds of the two species do not differ too much, both species can propagate with a similar waveform and speed, allowing mutualism to function as they travel, we name this scenario mutualistic propagation. Regimes (a), (b), and (c) correspond to the dynamics governed by $\mathbf{X_3} \to \mathbf{X_2} \to \mathbf{X_0}$, $\mathbf{X_3} \to \mathbf{X_0}$, and $\mathbf{X_3} \to \mathbf{X_1} \to \mathbf{X_0}$, respectively. The mutualistic propagation regime would be the best win-win situation [25] that can happen, where both species travel in synchrony to occupy regions with maximal population capacities. The steady wavefront propagating speeds for both species are shown in Fig. 7(d). The measured speeds are in excellent agreement with the prediction given in Sec. III. In the mutualistic propagation regime, both species travel with the same speed which has a kink at $v_1 = v_2$. Due to the presence of the mutualistic propagation regime the speed of each species has two kinks as v_1/v_2 increases, as shown in Fig. 7(c).

(IV) Predator-Prey, $0 < a_{\alpha\beta} < a_{\beta\beta}$ and $a_{\beta\alpha} < 0$: Here predator and prey are species β and species α, respectively. In this region, interspecific interaction of the prey to the predator is beneficiary while that of the predator on the prey is suppressing but not to strong to wipe out the prey to extinction. In the absence of diffusion, globally stable coexistence of the

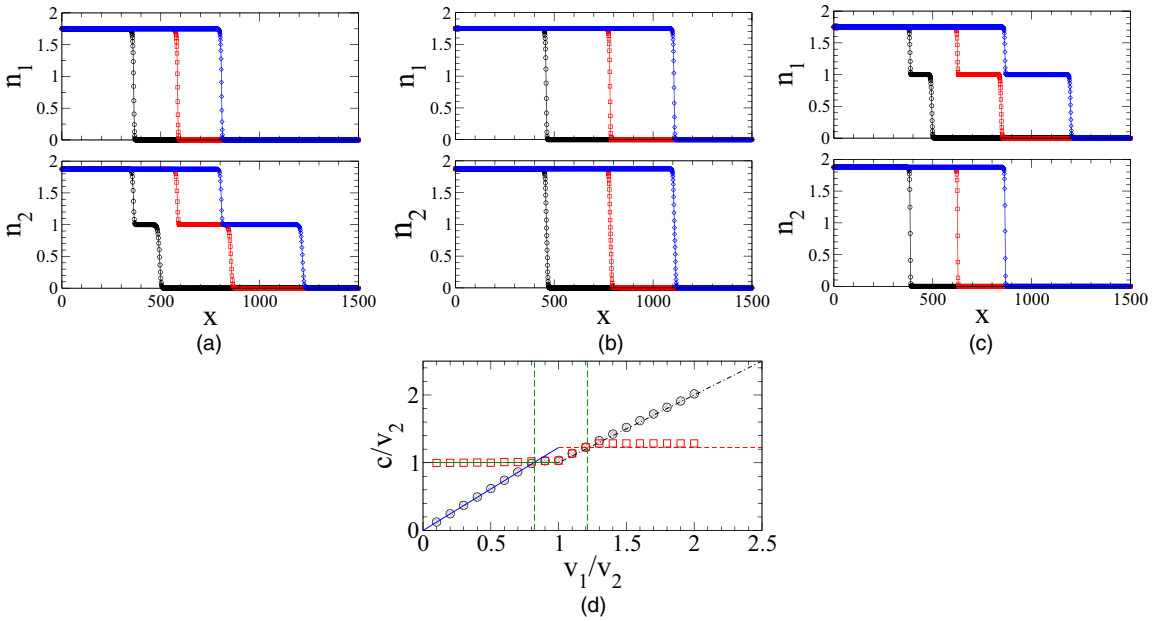

FIG. 7. Steady wavefront profiles in Regime III of the phase diagram Fig. 2 for (a) $v_1/v_2 = 1/2$, (b) $v_1/v_2 = 1/\sqrt{1.1}$ showing mutualistic propagation, (c) $v_1/v_2 = 2$. (d) Normalized wavefront speeds vs. the speed parameter ratio v_1/v_2. The mutualistic propagation regime is between the two vertical lines. Horizontal solid and dashed-dotted straight lines are the theoretical minimal speeds given in Eq. (9). Solid and horizontal dashed lines are the theoretical minimal speeds given in Eqs. (16) and (13), respectively. $a_{12}/a_{22} = -0.4$, $a_{21}/a_{11} = -0.5$. Symbols and units are the same as in Fig. 5.

two species results [see Figs. 1(d) and 3(d)]. The majority species at coexistence is the predator ($n_\alpha^* < n_\beta^*$) if $a_{\beta\beta} - a_{\alpha\beta} < a_{\alpha\alpha} + |a_{\beta\alpha}|$, and viceversa: if $a_{\beta\beta} - a_{\alpha\beta} > a_{\alpha\alpha} + |a_{\beta\alpha}|$, then the majority specie is the prey. Thus it is possible to have the coexistence population of the prey exceeds the predator only if $a_{\beta\beta} > a_{\alpha\alpha}$, i.e., the intraspecies competition of the prey is relatively low. However, if $a_{\beta\beta} \le a_{\alpha\alpha}$, the population of the predator will always dominate. In this case, the presence of species diffusion also allows for wave propagation, but the interplay of the intrinsic speeds can give rise to interesting scenarios. The wave profiles at different times for both species with species-1 and species-2 being the predator and prey respectively, are shown in Figs. 8(a)–8(c) corresponding to Regimes (a) $0 < \frac{v_1}{v_2} \le \frac{1}{\sqrt{1+\frac{|a_{12}|}{a_{22}}}}$, (b) $\frac{1}{\sqrt{1+\frac{|a_{12}|}{a_{22}}}} < \frac{v_1}{v_2} < 1$, and (c) $1 \le \frac{v_1}{v_2}$. Scenarios in Regimes (a), (b), and (c) correspond to the dynamics governed by $\mathbf{X_3} \to \mathbf{X_2} \to \mathbf{X_0}$, $\mathbf{X_3} \to \mathbf{X_0}$, and $\mathbf{X_3} \to \mathbf{X_1} \to \mathbf{X_0}$, respectively.

In Regime (a), although the population of the prey will be suppressed by the presence of the predator, the prey can escape to region free from predation if the intrinsic speed of the prey is faster. The wave profiles for such an "escape mode" is shown in Fig. 8(a) for $v_2 > v_1$ in which the leading edge of the prey is ahead of the predator's propagation and the prey can achieve its full population capacity. Interestingly, in this escape regime, there is a population spike at the leading edge of the predator's wavefront which is due to the increase in the population of the escaped prey that attract more predator. This can be interpreted as the effort of the predator in attempt to catch the escaping prey, but unsuccessfully.

Remarkably, the scenario of propagation in synchrony in Regime (b) occurs for a finite speed ratio regime for $v_1/v_2 \lesssim 1$, which can be interpreted as coexistence in "nomadic-pastoralism," namely, traveling tribes carrying along with their herd/cattle. Notice that there is also a small population spike for both species near their leading wavefront boundaries, suggesting the need of more predators to keep the prey from escaping to free regions. Finally, in Regime (c) the speed of the predator is faster than the prey, resulting in a portion of the faster predator in the leading edge of the wavefront along with a slower portion that travels with the same speed of the prey with the benefaction of a higher population capacity. The steady wavefront propagating speeds for both species are shown in Fig. 8(d) which are in excellent agreement with the predictions given in Sec. III. The region of nomadic-pastoralism propagation in synchrony (between two vertical dashed lines) is also indicated.

(V) [Subdivide into V^+ and V^-] One species dominating, $a_{\alpha\beta} > a_{\beta\beta}$ and $a_{\beta\alpha} < a_{\alpha\alpha}$: Here species β is the superior or dominating one and has a stronger interspecific competitive interaction than its intraspecific competition. The inferior (α species) competition on the superior ones is weak (weaker than its own intraspecific competition) and can even be beneficiary to the superior ones ($a_{\beta\alpha} < 0$ Regime V^- described below). In the absence of spatial diffusion, the dominating species will surely wipe out the inferior ones to extinction as indicated by the only stable fixed point in Fig. 1(e). But the above consequence can be quite different in the presence of diffusion in which steady wavefront propagation is allowed, the two populations can coexist but in different regions in some scenarios. In addition, the cases of $a_{\beta\alpha}$ being positive or negative can further be subdiveded into V^+ and V^-, respectively.

The wave profiles of the two species at three different times for V^+ ($a_{\beta\alpha} > 0$) are shown in Figs. 9(a) and 9(b), with species 1 being the superior one. The inferior species can survive if it

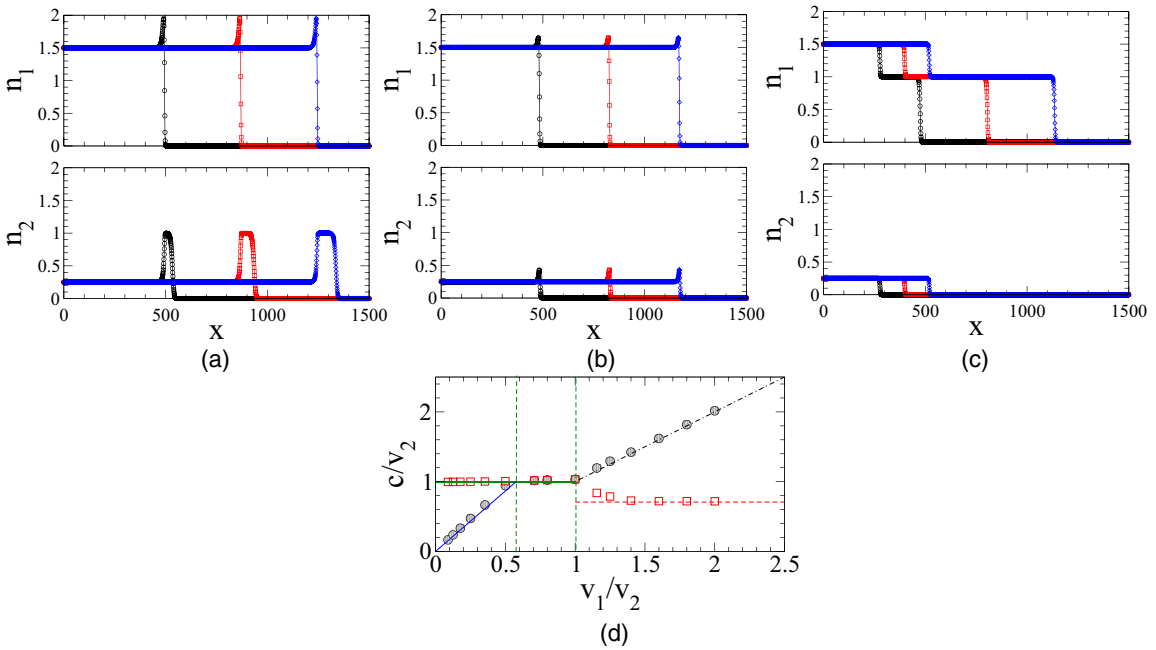

FIG. 8. Steady wavefront profiles in Regime IV of the phase diagram Fig. 2 for (a) $v_1/v_2 = 1/2$, (b) $v_1/v_2 = 1/\sqrt{1.25}$, (c) $v_1/v_2 = 2$. (d) Normalized wavefront speeds vs. the speed parameter ratio v_1/v_2. The nomadic-pastoralism regime is between the two vertical lines. Horizontal solid and dashed-dotted straight lines are the theoretical minimal speeds given in Eq. (9). Solid and horizontal dashed lines are the theoretical minimal speeds given in Eq. (16) and (13), respectively. $a_{12}/a_{22} = -2$, $a_{21}/a_{11} = 1/2$. Symbols and units are the same as in Fig. 5.

can outrun the superior to regions with its own species only. Such escape mode occurs when the intrinsic speed parameter of the inferior species exceeds that of the superior's, and the wave profile of the inferior consists of a fast leading front and a slow waveback with the same wave speed as the superior's. The dynamics of this escape mode can be described by the flow of $\mathbf{X_1} \to \mathbf{X_2} \to \mathbf{X_0}$. However, if the speed parameter of the superior species is faster, then the inferior species is wiped out to extinction everywhere, and the superior propagates with a speed given by its speed parameter [see Eq. (9)], as if the inferior species does not exist at all. In this extinction regime, the dynamics can be described by the flow $\mathbf{X_1} \to \mathbf{X_0}$. The steady wavefront propagating speeds for both species are shown in Fig. 9(c), which are in excellent agreement with the predictions given in Sec. III. Notice that there is also a "switch of gear" for the speed jump of

$$\delta c_1 = v_1\left(1 - \sqrt{1 - \frac{a_{12}}{a_{22}}}\right) \tag{18}$$

across $v_1 = v_2$ for the superior species.

For the case of V^- in which the inferior species is beneficiary to the superior ones, the wave propagations contain three different modes depending on their speed parameter ratios. The wave profiles at different times for both species are shown in Figs. 10(a)–10(c), corresponding to Regimes (a) $0 < \frac{v_1}{v_2} \le \frac{1}{\sqrt{1+\frac{|a_{12}|}{a_{22}}}}$, (b) $\frac{1}{\sqrt{1+\frac{|a_{12}|}{a_{22}}}} < \frac{v_1}{v_2} < 1$, and (c) $1 \le \frac{v_1}{v_2}$, respectively. Similar to the case of V^+, the fast intrinsic speed of the inferior species results in the escape mode in Regime (a) in which the inferior species propagates with a fast wavefront

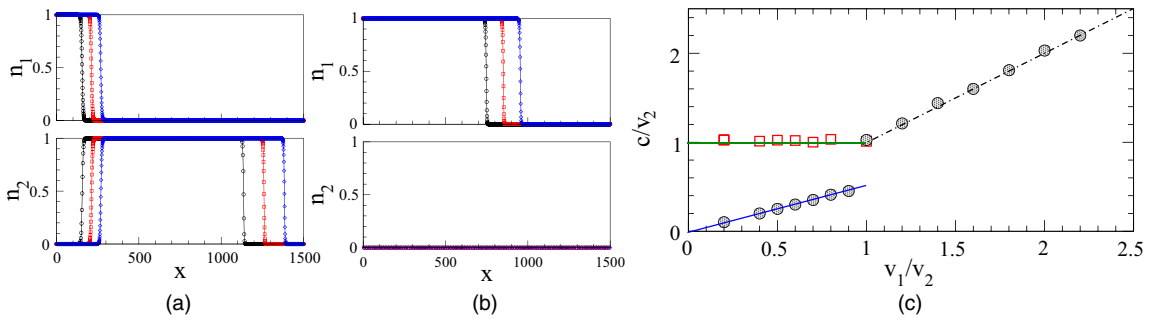

FIG. 9. Steady wavefront profiles in Regime V^+ (species-1 is the dominating/superior species) of the phase diagram Fig. 2 for (a) $v_1/v_2 = 1/2$, (b) $v_1/v_2 = 2$. (c) Normalized wavefront speeds vs. the speed parameter ratio v_1/v_2. Horizontal solid and dashed-dotted straight lines are the theoretical minimal speeds given in Eq. (9). Solid line is the theoretical minimal speeds given in Eq. (16). $a_{12}/a_{22} = 3/4$, $a_{21}/a_{11} = 5/4$. Symbols and units are the same as in Fig. 5.

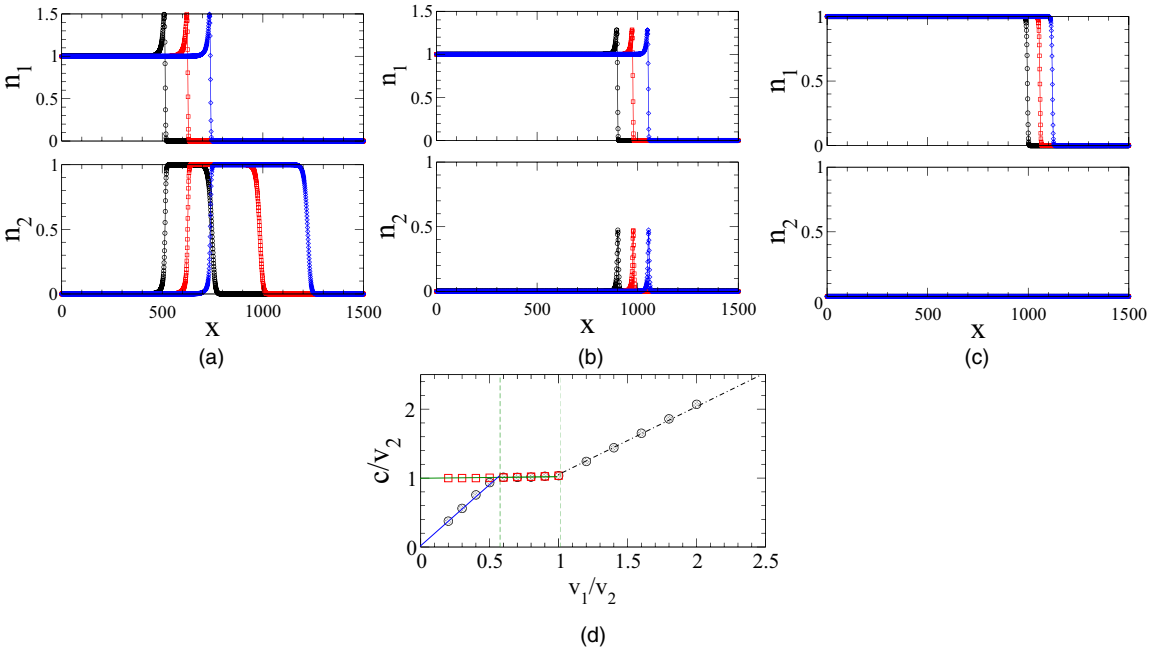

FIG. 10. Steady wavefront profiles in Regime V^- of the phase diagram Fig. 2 for (a) $v_1/v_2 = 1/4$, (b) $v_1/v_2 = 4/5$, (c) $v_1/v_2 = 2$. (d) Normalized wavefront speeds vs the speed parameter ratio v_1/v_2. The co-propagating regime is between the two vertical lines. Horizontal solid and dashed-dotted straight lines are the theoretical minimal speeds given in Eq. (9). Solid line is the theoretical minimal speeds given in Eq. (16). $a_{12}/a_{22} = -2$, $a_{21}/a_{11} = 5/4$. Symbols and units are the same as in Fig. 5.

and a slower waveback of the same speed as the wavefront of the superior species. It corresponds to the dynamics governed by $\mathbf{X_1} \to \mathbf{X_2} \to \mathbf{X_0}$. However, the escape mode in V^- has a distinct population spike of the superior species in the leading edge of the wave front, which is similar to that of the escape mode in Regime IV [see Fig. 8(a)] for similar reasons. If the superior species has a faster intrinsic speed, then the inferior species will be driven to extinction, similar to V^+. Contrary to V^+, in V^- there exists a finite range of intrinsic speed ratios [Fig. 10(b)], such that both species co-propagate with the same wave speeds. Scenarios in (b) and (c) correspond to the dynamics of $\mathbf{X_1} \to \mathbf{X_0}$. The steady wave speeds are measured (symbols) together with the theoretical predictions (lines) are shown in Fig. 10(d), showing excellent agreement. Notice that contrary to V^+, there is no abrupt speed jump here as the speed parameter is varied.

(VI) Strong mutualism, $a_{\alpha\beta} < 0$ and $\det \mathbf{a} < 0$: In this case, the mutual benefaction is too strong in boosting mutual growth that leads to population explosion. The intra-competitions of the species are not enough to suppress the enhanced growth due to strong mutualistic interactions and the populations of both species will diverge rapidly.

V. DISCUSSIONS AND BIOLOGICAL RELEVANCE

In this paper, the population dynamics and wave properties for the two-species LV model with general interaction parameters are classified in term of a phase diagram. Each regime in the phase diagram has its own biological implications as indicated by its name. Wave propagation solutions exist in general allowing for efficient directional species movement. In this section, we summarize our findings with possible extensions or outlooks, and further discuss the relevant biological or ecological implications of our results.

A. Summary and outlook

Out results are conveniently summarized by the phase diagram in (Fig. 2). In these different regimes, the steady wavefront propagating speeds for both species are examined as functions of their speed parameters by measuring the wave speeds from the numerical solutions of Eq. (2) for waves that have attained their steady shapes. The wavefront speeds are well predicted by minimal speed values from the analytic results given by Eqs. (9), (13), and (16) in Sec. III. The wave speeds depend on both the interaction parameters $a_{\alpha\beta}$ and the intrinsic speed parameters v_α. The intrinsic speed parameter, which is determined by both the species growth rate and its diffusive mobility, plays a decisive role in the fate of the population survival and territory occupation. In many situations, the nature of the propagating waves show a sharp change as v_1 increases across v_2 suggesting a "switch of gear" mechanism of effective changing in speeds by employing the nonlinear dynamical properties.

Our results indicated that diffusion or motility of the species can strongly alter the spatiotemporal dynamics, which is also observed for other related dynamical models, including spatiotemporal patterns described by the complex Ginzburg-Landau equation [14,15], the mobility-induced enhancement or breakdown of cooperation in replicator dynamics [17,29,30], and in the spatial patterns formed in prisoner's dilemma models [16,31,32]. The present study of the general two-species interaction LV model is not restricted to specific model parameters and provides a connection

between different models. The cause of the wave dynamics in the present work is mainly due to the front-propagation into unstable states [33], or the so-called the "pulled-front" propagations, while it may be of different mechanisms for the complex spatiotemporal patterns occurring in other dynamical systems. For instance, in the phenomenological quintic Ginzburg-Landau equation (e.g., in first-order phase transition) or Swift-Hohenberg equation, depending on the parameters or nonlinearity, both pulled and pushed fronts with different velocity selection rules are possible [15].

The present study focused on the case of one spatial dimension but motions in two and three spatial dimensions, respectively, are needed for organisms that live on land/shallow water and in ocean or in air. And for the two-dimensional generalization of Eq. (2), it can be shown, similar to the case of the standard Fisher-Kolmogorov-Petrovskii-Piscounov equation [34], that the asymptotic radial symmetric solution admits a propagating wavefront solution with speed limits given by the one-dimensional results. Thus, one anticipates the conclusion in the present work would still hold for weakly curved fronts in higher spatial dimensions, or for radially and spherical symmetric cases. However, transverse instability could result in breaking the radial symmetry resulting in complex spatiotemporal (nonlinear) patterns that destroys the simple propagating wavefronts. More detail analytical and numerical studies can be carried out to investigate systems in higher dimensions.

The dynamics considered here is purely deterministic without taking into account of possible environmental or intrinsic fluctuations. However, different microscopic dynamical models, such as birth-coagulation reaction-diffusion model or directed percolation model, can lead to different forms of multiplicative noises. Such noises can also be included resulting in stochastic partial differential equations, which can be investigated systematically using similar approaches for the stochastic Fisher-Kolmogorov-Petrovskii-Piscounov (sFKPP) equations [35,36]. It has been shown that the propagating Fisher wavefronts are still robust in the presence of noises [36,37] in the sFKPP model, with the wave speed being modified differently in the weak noise [38] and strong noise [39] limits. Thus one anticipates that waves found in the present model should also be robustunder noises, and some analytical results for the wavefront speeds could be obtained. However, more thorough analytical and numerical studies should be carried out to investigate the dynamics of the LV model under various types of noises.

B. Biological and ecological implications

From the viewpoint of biodiversity, species coexistence is essential for ecological balance. From the results in the LV model, two species can coexist in the same spatial domain by three pathways: (weak) competitive coexistence, (weak) mutualistic coexistence, and predator-prey coexistence, corresponding to Regimes II, III, and IV in the phase diagram. The global stability is confirmed by the explicit Lyapunov functions, and such stable coexistence persists also in the presence of spatial diffusion. In addition, in Regimes III and IV, there is a special copropagating region in which both species propagate through with the same wave speed, and thus sustaining maximal coexistence and biodiversity in space and time. In addition, one can interpret our results in various regimes of the phase diagram in terms of the relevance or implications in biology, ecology, and population development strategy, which will be discussed below.

The scenario in Regime II can be thought of as the process of wound healing [40], in which old healthy cells (species 2) and newly proliferated cells (species 1) compete for resources but can coexist persistently. Old cells have less competitive effect on the newly proliferated cells so as to assist the growth of new cells and is modeled by the condition of $a_{12} < a_{21}$. When there is a wound, the epidermal cell will begin its fast proliferation and undergoes migration. The old healthy cells will then reduce their growth rates (r_2) such that the condition $v_2 < v_1$ is reached. The newly proliferated cells can then propagate with a fast speed of c_1 while the old cells with a slow speed of c_2 [see Fig. 6(b)]. Remarkably, the system can exploit the dynamical behavior of "shift of gear" to boost the speed of the new cells by δc_1 and a speed drop of the old cells by δc_2 for efficient adjustment of the cell movement speeds across $v_2 = v_1$, as described in Sec. IV.

The weak mutualistic interactions in Regime III can enhance bio-diversity due to its stable species coexistence. Many symbiotic ecological systems can be modeled by this scenario, such as plants and pollinators/seed dispersers. In the presence of species mobility, weak mutualism is essential for coevolution and maintaining a stable population while at the same time both species can occupy new territories by efficient wave propagations. In the case that the mutualism between the two species is obligate, i.e., one cannot survive without the other, then two species moving with the same speeds in synchrony is critical. Remarkably, our result indicated such a copropagating wave with the same speed is feasible (without fine tuning) in a finite parameter range of the intrinsic speeds, as given by region (b) in Fig. 7. One can further examine the population growth rates of both species under steady wave propagations. Direct calculations give

$$\frac{dN_1}{dt} = c_1^{\min} n_1^*,$$
$$\frac{dN_2}{dt} = c_1^{\min} n_2^* + \frac{v_2 - c_1^{\min}}{a_{22}} \quad \text{in region III(a)}, \tag{19}$$
$$\frac{dN_1}{dt} = n_1^* \mathrm{Max}(v_1, v_2),$$
$$\frac{dN_2}{dt} = n_2^* \mathrm{Max}(v_1, v_2) \quad \text{in region III(b)}, \tag{20}$$
$$\frac{dN_1}{dt} = c_2^{\min} n_1^* + \frac{v_1 - c_2^{\min}}{a_{11}},$$
$$\frac{dN_2}{dt} = c_2^{\min} n_2^* \quad \text{in region III(c)}, \tag{21}$$

where $c_1^{\min} \equiv \sqrt{1 - a_{12}/a_{22}}\, v_1$ and $c_2^{\min} \equiv \sqrt{1 - a_{21}/a_{11}}\, v_2$ are the minimal speeds given by Eqs. (16) and (13), respectively. Figure 11 shows the population growth rates of both species as a function of one of the species' speed parameter while the speed parameter of the other species is fixed. As the speed parameter of one of the species increases, not only its own growth rate increases, the growth rate of the other species can also increase

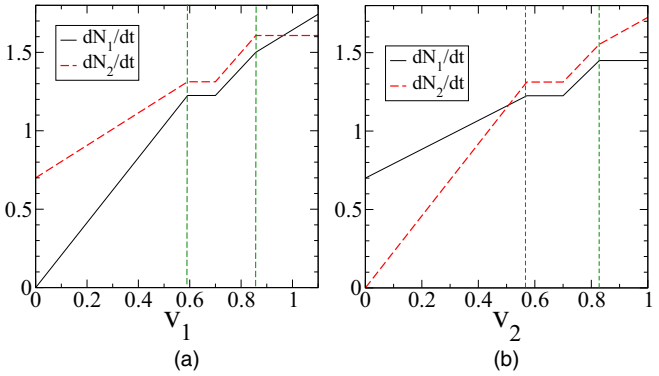

FIG. 11. Steady population growth rates in Regime III as a function of (a) speed parameter v_1 for fixed $v_2 = 0.7$, (b) speed parameter v_2 for fixed $v_1 = 0.7$. Region in which waves of both species are propagating in synchrony with the same speed is denoted between two vertical dashed-lines. Other parameters are the same as in Fig. 7.

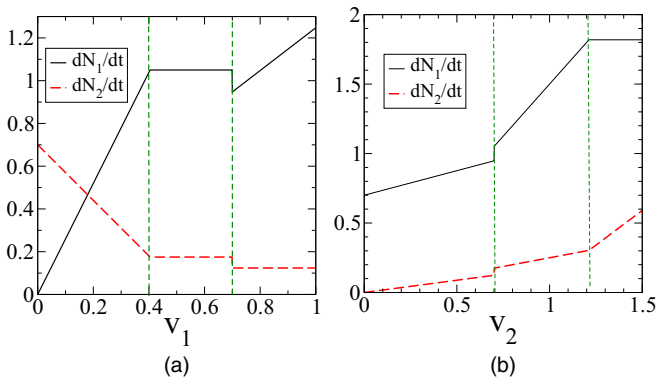

FIG. 12. Steady population growth rates in Regime IV as a function of (a) predator's speed parameter v_1 for fixed $v_2 = 0.7$, (b) prey's speed parameter v_2 for fixed $v_1 = 0.7$. Region in which waves of the predator and prey are propagating in synchrony with the same speed is denoted between two vertical dashed-lines. Other parameters are the same as in Fig. 8.

due to mutualistic interactions as shown in the small v_1 region in Fig. 11(a) and small v_2 region in Fig. 11(b). There are also regimes in which the growth rate of the other species remains unchanged (the advantage of mutualism is not utilized), as in the large v_1 region in Fig. 11(a) and large v_2 region in Fig. 11(b). In the copropagating region in which both species are traveling with the same speed, one might anticipate the species can take full advantage of mutualism to boost the populations, but this is not so, as depicted by a local concave region in the growth rates in this regime as shown in Fig. 11. This is because in this copropagating regime, both species achieve high population densities n_1^* and n_2^* and the mutualistic interactions are not strong enough (weak mutualism, $a_{12}a_{21} < a_{11}a_{22}$) to counteract the strong intraspecies competitions which suppress the growth rate. It is worth to note that there is a constant growth rate region for both species within the copropagating regime. Such a regime would be very suitable for stable development since both species can maintain a robust growth rate upon (small) external perturbations or internal fluctuations on the parameters of the system.

In the absence of species mobility, Regime IV of predator-prey can also model the parasite-host coexistence. However, parasites always stuck with their host and cannot be detached, thus diffusive model is not suitable for modeling of such a situation. There are numerous predator-prey systems that possess spatial mobility for animals in land and sea, also for bacteria and single cell organisms. The diffusive predator-prey model is important for modeling territorial ecology associated with food chains. The population growth rates of both species under steady wave propagations are given by

$$\begin{aligned} \frac{dN_1}{dt} &= c_1^{\min} n_1^*, \\ \frac{dN_2}{dt} &= c_1^{\min} n_2^* + \frac{v_2 - c_1^{\min}}{a_{22}} \qquad \text{in region IV(a)}, \end{aligned} \tag{22}$$

$$\begin{aligned} \frac{dN_1}{dt} &= n_1^* v_2, \\ \frac{dN_2}{dt} &= n_2^* v_2 \qquad \text{in region IV(b)}, \end{aligned} \tag{23}$$

$$\begin{aligned} \frac{dN_1}{dt} &= c_2^{\min} n_1^* + \frac{v_1 - c_2^{\min}}{a_{11}}, \\ \frac{dN_2}{dt} &= c_2^{\min} n_2^* \qquad \text{in region IV(c)}. \end{aligned} \tag{24}$$

Figure 12 shows the population growth rates of both predator and prey as a function of one of the species' speed parameter while the speed parameter of the other species is fixed. As the intrinsic speed parameter of the predator increases, there is a plateau region for the predator growth rate corresponding to the copropagating regime of both species traveling with the same speed and the growth rate of the prey also stays constant in this regime [see Fig. 12(a)]. The plateau or local maximum in the predator's growth rate indicates that the predators are taking advantage of propagating with the same speed as their prey. However, in the copropagating regime, both growth rates increase with the intrinsic speed parameter of the prey [see Fig. 12(b)]. As mentioned before, one can interpret the equal speed copropagating regime as nomadic-pastoralism, thus the constant population growth rates in this regime [see Fig. 12(a)] suggest the system is highly robust against perturbations in the changes of the parameters of the nomadic (species 1), but the growth rates are more sensitive (proportional) to the intrinsic speed parameter of the pastoral (species 2), as given by Eq. (23). Therefore, in order to sustain a stable environment for development, the nomadic should maintain a low population (small n_1^*) so that their growth rate will not be too sensitive to the variation of the parameters of the pastoral. This can be achieved by maintaining a low intracompetitive environment for the pastoral (i.e., small a_{22}, since $n_1^* = (a_{22} + |a_{12}|)/\det \mathbf{a}$), and also keeping the environment (parameters) of the pastoral as stable as possible. In addition, a smaller value of a_{22} will also broaden the copropagating regime and enhance the robustness.

In the one-species dominating Regime V^+ (shown in Fig. 9), there is an abrupt jump in the wavefront speed of the superior species as its speed parameter exceeds that of the inferior species, as given by Eq. (18). This scenario can be thought of analogous to the process of cancer development characterised

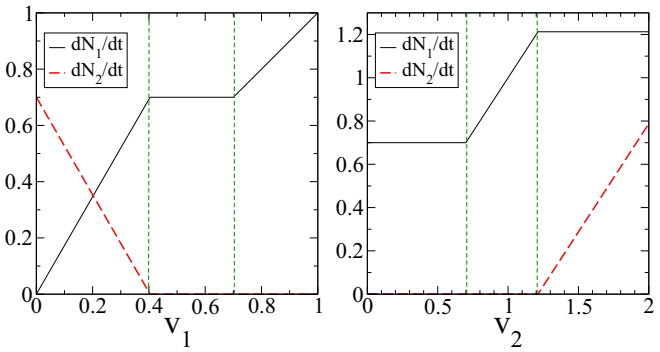

FIG. 13. Steady population growth rates in Regime V$^-$ as a function of (a) speed parameter v_1 for fixed $v_2 = 0.7$, (b) speed parameter v_2 for fixed $v_1 = 0.7$. Region in which waves of both species are propagating in synchrony with the same speed is denoted between two vertical dashed-lines. Other parameters are the same as in Fig. 10.

by the uncontrolled growth and fast dispersal of cancer [41,42]. One can think of the cancer cells as the dominating or superior species in the sense that they have strong competition on the (inferior) normal cells. The normal cells have stronger intracompetition due to apoptosis but the cancer cells have stronger intercompetition to disturb the normal cells. The case of low speed parameter ($v_1 < v_2$ region in Fig. 9) can be thought of as benign cancerous tumor cells in which they can proliferate but migrate with a slow speed and healthy cells can still grow. In the metastasis stage, the proliferation and/or migration of the cancer cells become active and its speed parameter increases. As its speed parameter exceeds that of the normal cells, there is a sharp increase in the propagation speed of the cancer cells by a factor of $1/\sqrt{1-a_{12}/a_{22}}$, and at the same time the cancer cells will occupy all the possible resources and suppress the growth of normal cells.

However, there is no sharp jump or drop in the wave speed in the V$^-$ region as the intrinsic speed parameter changes, but there is a finite region of co-propagation in which both species have the same wave speeds [see Figs. 10(b) and 10(d)]. The steady population growth rates of both species under steady wave propagation are given by

$$\frac{dN_1}{dt} = \frac{c_1^{\min}}{a_{11}} \quad \frac{dN_2}{dt} = \frac{v_2 - c_1^{\min}}{a_{22}} \quad \text{in region V}^-\text{(a)}, \tag{25}$$

$$\frac{dN_1}{dt} = \frac{v_2}{a_{11}} \quad \frac{dN_2}{dt} = 0 \quad \text{in region V}^-\text{(b)}, \tag{26}$$

$$\frac{dN_1}{dt} = \frac{v_1}{a_{11}}, \quad \frac{dN_2}{dt} = 0 \quad \text{in region V}^-\text{(c)}. \tag{27}$$

The population growth rates of both superior and inferior species as a function of one of the species' speed parameter while the speed parameter of the other species is fixed are shown in Fig. 13. As the intrinsic speed parameter of the superior species (species 1) increases, its growth rate increases at the expense of the inferior's (species 2) and eventually extinguish the growth rate of the inferior species in the co-propagating region [see Fig. 13(a)]. The growth rate of the dominating species stays constant inside the co-propagating region and therefore is robust against variations in its parameters, which is desirable for stable development of the superior species. In the copropagating region, the inferior species can only sustain a small finite population with a vanishing growth rate. The inferior species can only grow if its intrinsic speed parameter can evolve to exceed that of the superior species [see Fig. 12(b)], however as v_2 increases to the copropagating region, the superior species can take advantage and accelerates its growth rate. The inferior species can only escape the domination if it can outrun the superior species in the $v_2 > v_1$ regime.

ACKNOWLEDGMENTS

This work has been supported by the Ministry of Science and Technology of Taiwan under Grant No. MOST104-2112-M-008-003-MY3, NCTS of Taiwan, and NSFC of China under Grant No. 11204132.

APPENDIX: DERIVATION OF LYAPUNOV FUNCTION FOR SPECIES COEXISTENCE

Here we are interested in the species coexisting regimes whose stability can be guaranteed by the existence of a Lyapunov function. Nontrivial coexistence fixed point $n_1^* > 0$ and $n_2^* > 0$ exists in Regimes I, II, III, and IV. Furthermore, notice that the determinant, $\det \mathbf{a} = a_{11}a_{22} - a_{12}a_{21} > 0$ holds in these regimes.

For the case of positive a_{12} and a_{21}, it has been shown [43] that an energy or fittnesslike Lyapunov function of the form

$$V_{\text{fit}}(n_1,n_2) = \tfrac{1}{2}D_1a_{11}n_1^2 + \tfrac{1}{2}D_2a_{22}n_2^2 + \tfrac{1}{2}(D_1a_{12} + D_2a_{21})n_1n_2 - D_1n_1 - D_2n_2 \tag{A1}$$

exists, where $D_1, D_2 > 0$. One can show by direct calculation that

$$\dot{V}_{\text{fit}} = \frac{\partial V_{\text{fit}}}{\partial n_1}\dot{n}_1 + \frac{\partial V_{\text{fit}}}{\partial n_2}\dot{n}_2 \tag{A2}$$

$$= -r_1n_1D_1(a_{11}\delta n_1 + a_{12}\delta n_2)^2 - r_2n_2D_2(a_{21}\delta n_1 + a_{22}\delta n_2)^2 + \frac{n_1n_2}{2}(D_1a_{12} - D_2a_{21})[r_1(a_{11}\delta n_1 + a_{12}\delta n_2) - r_2(a_{21}\delta n_1 + a_{22}\delta n_2)], \tag{A3}$$

where $\delta n_i \equiv n_i - n_i^*$ is the deviation from the coexistence fixed point. Hence, a suitable choice to guarantee $\dot{V}_{\text{fit}} \le 0$ would be $D_1a_{12} = D_2a_{21}$, which was employed in Ref. [44] with $D_1 = a_{21} > 0$ and $D_2 = a_{12} > 0$. It can be easily seen that V_{fit} can serve as a Lyapunov function if $a_{12}a_{21} > 0$, i.e., in Regimes I, II, and III ($D_1 = |a_{21}|$, $D_2 = |a_{12}|$), but not so for the case $a_{12}a_{21} < 0$ [Regime IV].

To overcome the above difficulty, here we propose an entropylike Lyapunov function of the form [2]

$$V(n_1,n_2) = A(n_1 - n_1^* \ln n_1) + B(n_2 - n_2^* \ln n_2), \tag{A4}$$

which is legitimate in all regimes, where the constants A and B are to be determined. Direct calculation

gives

$$\dot{V} = \frac{\partial V}{\partial n_1}\dot{n}_1 + \frac{\partial V}{\partial n_2}\dot{n}_2 = -\frac{1}{2}\delta\vec{n}^T\mathbf{M}\delta\vec{n}, \tag{A5}$$

$$\mathbf{M} \equiv \begin{pmatrix} 2Ar_1a_{11} & Ar_1a_{12} + Br_2a_{21} \\ Ar_1a_{12} + Br_2a_{21} & 2Br_2a_{22} \end{pmatrix}. \tag{A6}$$

For Lyapunov function, one requires $\dot{V} < 0$ everywhere except at the coexistence fixed point at which $\dot{V}(n_1^*, n_2*) = 0$. The eigenvalues of $\mathbf{M}$ need to be positive for $\dot{V} < 0$ to hold, thus one has

$$\mathrm{Tr}\,\mathbf{M} = 2(Ar_1a_{11} + Br_2a_{22}) > 0, \tag{A7}$$

$$\det\mathbf{M} = 4ABr_1r_2a_{11}a_{22} - (Ar_1a_{12} + Br_2a_{21})^2 > 0. \tag{A8}$$

Since both $a_{11}, a_{22} > 0$, one must have $A > 0$ and $B > 0$. $\det\mathbf{M}$ can also be written as

$$\det\mathbf{M} = 4ABr_1r_2\det\mathbf{a} - (Ar_1a_{12} - Br_2a_{21})^2. \tag{A9}$$

Notice that since $\det\mathbf{a} > 0$ in these regimes and hence the first terms in the right-hand side of both Eqs. (A8) and (A9) are positive. Thus, if one can choose $A > 0$ and $B > 0$ such that the second term in the right-hand side of either Eq. (A8) or (A9) to vanish will guarantee $\det\mathbf{M} > 0$ and hence a Lyapunov function is constructed. It is easy to verify by direct inspection that $A = r_2|a_{21}|$ and $B = r_1|a_{12}|$ is a legitimate choice for stable coexistence in Regimes II, III, and IV. To incorporate the unstable coexistence populations in Regime I, the Lyapunov function can be modified to

$$V(n_1,n_2) = r_2\mathrm{sgn}(a_{11} - a_{21})|a_{21}|(n_1 - n_1^*\ln n_1) + r_1\mathrm{sgn}(a_{22} - a_{12})|a_{12}|(n_2 - n_2^*\ln n_2), \tag{A10}$$

which is valid for all the cases of species coexistence in Regimes I, II, III, and IV.

To examine whether the above stability properties will be altered when spatial diffusion is taken into account in the PDE system Eq. (2), one can construct the following Lyapunov functional:

$$\mathscr{V}(t) \equiv \int V(n_1(x,t),n_2(x,t))dx. \tag{A11}$$

Using Eqs. (2) and Green's identity (integration by parts), one obtains

$$\dot{\mathscr{V}} = \int\left(\frac{\partial V}{\partial n_1}\frac{\partial n_1}{\partial t} + \frac{\partial V}{\partial n_2}\frac{\partial n_2}{\partial t}\right)dx \tag{A12}$$

$$= \int \dot{V}dx - \partial_x\vec{n}^T\begin{pmatrix} d_1 & 0 \\ 0 & d_2 \end{pmatrix}\begin{pmatrix} \frac{\partial^2 V}{\partial n_1^2} & \frac{\partial^2 V}{\partial n_1\partial n_2} \\ \frac{\partial^2 V}{\partial n_1\partial n_2} & \frac{\partial^2 V}{\partial n_2^2} \end{pmatrix}\partial_x\vec{n}, \tag{A13}$$

where $\partial_x\vec{n}^T \equiv (\partial_x n_1, \partial_x n_2)$. Lyapunov stability of the homogeneous coexistence steady-state ($\dot{V} \le 0$) guarantees the first term in Eq. (A13) to be nonpositive. And if the Hessian matrix of V is further shown to be semipositive definite, then one has $\dot{\mathscr{V}} \le 0$ establishing the stability of the Lyapunov functional. For the Lyapunov function of the form in Eq. (A4), the Hessian matrix is diagonal with elements $(An_1^*/n_1^2, Bn_2^*/n_2^2)$, and hence the Lyapunov functional for the reaction diffusion system Eq. (2) has the same stability as the time-independent ODE system Eq. (1), namely, the two-species coexistence is unstable in Regime I, but stable in Regimes II, III, and IV.

[1] A. J. Lotka, Contribution to the theory of periodic reaction, J. Phys. Chem. **14**, 271 (1910); Analytical note on certain rhythmic relations in organic systems, Proc. Natl. Acad. Sci. USA **6**, 410 (1920).

[2] V. Volterra, in *Variations and Fluctuations of the Number of Individuals in Animal Species Living Together in Animal Ecology*, edited by R. N. Chapman (McGraw-Hill, New York, 1931).

[3] N. S. Goel *et al.*, *On the Volterra and Other Nonlinear Models of Interacting Populations* (Academic Press, San Diego, 1971).

[4] H. I. Freedman, *Deterministic Mathematical Models in Population Ecology* (Marcel Dekker, New York 1980).

[5] F. Brauer and C. Castillo-Chavez, *Mathematical Models in Population Biology and Epidemiology* (Springer-Verlag, New York 2000).

[6] J. Maynard-Smith, *Evolution and the Theory of Games* (Cambridge University Press, Cambridge, UK, 1982).

[7] J. W. Weibull, *Evolutionary Game Theory* (MIT Press, Cambridge, MA, 1995).

[8] J. Hofbauer and K. Sigmund, *Evolutionary Games and Population Dynamics* (Cambridge University Press, Cambridge, 1998).

[9] T. C. Gard and T. G. Hallam, Persistence in food webs—Lotka-Volterra food chains, Bull. Math. Biol. **41**, 877 (1979).

[10] I. Bomze, Lotka-Volterra equation and replicator dynamics: A two-dimensional classification, Biol. Cybern. **48**, 201 (1983); Lotka-Volterra equation and replicator dynamics: New issues in classification, **72**, 447 (1995).

[11] J. Hofbauer, T. V. Hutson, and G. T. VickersTravelling waves for games in economics and biology, Nonlin. Anal. Theory Methods Appl. **30**, 1235 (1997).

[12] A. Agranovich and Y. Louzoun, Predator-prey dynamics in a uniform medium lead to directed percolation and wave-train propagation, Phys. Rev. E **85**, 031911 (2012).

[13] C. P. Rocaa, J. A. Cuesta, and A. Sanchez, Evolutionary game theory: Temporal and spatial effects beyond replicator dynamics, Phys. Life Rev. **6**, 208 (2000).

[14] M. C. Cross and P. C. Hohenberg, Pattern formation out of equilibrium, Rev. Mod. Phys. **65**, 851 (1993).

[15] W. van Saarloos and P. C. Hohenberg, Fronts, pulses, sources, and sinks in generalized complex Ginzburg-Landau equations, Physica D **56**, 303 (1992).

[16] S. Amadae, *"Prisoner's Dilemma," Prisoners of Reason* (Cambridge University Press, New York, 2016).

[17] M. H. Vainstein and J. J. Arenzon, Spatial social dilemmas: Dilution, mobility, and grouping effects with imitation dynamics, Physica A **394**, 145 (2014).

[18] M. M. Tang and P. C. Fife, Propagating fronts for competing species equations with diffusion, Arch. Ration. Mech. Anal. **73**, 69 (1980).

[19] R. A. Gardner, Existence and stability of traveling wave solutions of competition models: A degree theoretic approach, J. Diff. Equ. **44**, 343 (1982).

[20] R. A. Gatenby, Models of tumor host interaction as competing populations|Implications for tumor biology and treatment, J. Theor. Biol. **176**, 447 (1995); Application of competition theory to tumour growth: Implications for tumour biology and treatment, Eur. J. Cancer, Part A **32**, 722 (1996).

[21] Y. Kan-On, Parameter dependence of propagation speed of traveling waves for competition-diffusion equations, SIAM J. Math. Anal. **26**, 340 (1995); Y. Kan-on, Fisher wavefronts for the Lotka-Volterra competition model with diffusion, Nonlin. Anal. Theory Methods Appl. **28**, 145 (1997).

[22] J. I. Kanel and L. Zhou, Existence of wave front solutions and estimates of wave speed for a competition-diffusion system, Nonlin. Anal. Theory Methods Appl. **27**, 579 (1996).

[23] Y. Hosono, The minimal speed of traveling fronts for a diffusive Lotka-Volterra competition model, Bull. Math. Biol. **60**, 435 (1998); Singular perturbation analysis of traveling waves for diffusive Lotka-Volterra competitive models, in *Numerical and Applied Mathematics Part II* (Baltzer, Basel, 1989).

[24] M. X. Wang and P. Y. Lai, Population dynamics and wave propagation in Lotka-Volterra system with spatial diffusion, Phys. Rev. E **86**, 051908 (2012).

[25] M. X. Wang and Y. Ma, Population evolution in mutualistic Lotka-Volterra system with spatial diffusion, Physica A **395**, 228 (2014).

[26] R. A. Fisher, The wave of advance of advantageous genes, Ann. Eugenics **7**, 355 (1937); A. Kolmogorov, I. Petrovskii, and N. Piscounov, A study of the diffusion equation with increase in the amount of substance, and its application to a biological problem, in *Selected Works of A. N. Kolmogorov I*, edited by V. M. Tikhomirov (Kluwer, Dordrecht, 1991), pp. 248–270.

[27] M. X. Wang, Y. J. Li, P. Y. Lai, and C. K. Chan, Model on Cell migration, Growth, differentiation and de-differentiation: Reaction-Diffusion Equation and Wave propagation, Euro. J. Phys. E **36**, 65 (2013).

[28] M. X. Wang, P. Y. Lai, and Y. Ma, Regulatory effects on the population dynamics and wave propagation in a cell lineage model, J. Theor. Biol. **393**, 105 (2016).

[29] M. Enquistand and O. Leimar, The evolution of cooperation in mobile organisms, Physica A **45**, 747 (1993).

[30] J. Gómez-Gardeñes, M. Campillo, L. M. Floría, and Y. Moreno, Dynamical Organization of Cooperation in Complex Topologies, Phys. Rev. Lett. **98**, 108103 (2007).

[31] A. Szolnoki, Z. Wang, J. Wang, and X. Zhu, Dynamically generated cyclic dominance in spatial prisoner's dilemma games, Phys. Rev. E **82**, 036110 (2010).

[32] A. Szolnoki and M. Perc, Costly hide and seek pays: Unexpected consequences of deceit in a social dilemma, New J. Phys. **16**, 113003 (2014); Evolutionary dynamics of cooperation in neutral populations, **20**, 013031 (2018).

[33] W. Van Saarloos, Front propagation into unstable states, Phys. Rep. **386**, 29 (2002).

[34] J. D. Murray, *Mathematical Biology*, 3rd ed. (Springer, New York, 2002).

[35] C. Mueller and R. Tribe, Stochastic PDEs arising from the long range contact and long range voter processes, Prob. Theory Relat. Fields **102**, 519 (1995).

[36] C. R. Doering, C. Mueller, and P. Smereka, Interacting particles, the stochastic Fisher-Kolmogorov-Petrovsky-Piscounov equation, and duality, Physica A **325**, 243 (2003).

[37] C. Kuehn, Warning signs for wave speed transitions of noisy Fisher-KPP invasion fronts, Theor. Ecol. **6**, 295 (2013).

[38] E. Brunet and B. Derrida, Shift in the velocity of a front due to a cutoff, Phys. Rev. E **56**, 2597 (1997).

[39] O. Hallatschek and K. S. Korolev, Fisher Waves in the Strong Noise Limit, Phys. Rev. Lett. **103**, 108103 (2009).

[40] M. Poujade *et al.*, Collective migration of an epithelial monolayer in response to a model wound, Proc. Natl. Acad. Sci. USA **104**, 15988 (2007).

[41] L. Liu *et al.*, Probing the invasiveness of prostate cancer cells in a 3D microfabricated landscape, Proc. Natl. Acad. Sci. USA **108**, 6853 (2011).

[42] J. Y. Chang and P. Y. Lai, Uncontrolled growth resulting from dedifferentiation in a skin cell proliferation model, Phys. Rev. E **85**, 041926 (2012).

[43] R. H. MacArthur, Species packing, and what competition minimizes, Proc. Natl. Acad. Sci. USA **64**, 1369 (1969).

[44] Y. Tang, R. Yuan, and Y. Ma, Dynamical behaviors determined by the Lyapunov function in competitive Lotka-Volterra systems, Phys. Rev. E **87**, 012708 (2013).